

# SNHG8 is identified as a key regulator in non-small-cell lung cancer progression sponging to miR-542-3p by targeting CCND1/CDK6

Changhao Chen<sup>1,\*</sup>Zhiwei Zhang<sup>2,\*</sup>Jie Li<sup>3</sup>Yuejun Sun<sup>4</sup>

<sup>1</sup>Department of General Surgery, The Second Hospital of Nanjing, Nanjing University of Chinese Medicine, Nanjing, Jiangsu 210003, China;

<sup>2</sup>Department of Cardiothoracic Surgery, The Second Affiliated Hospital of Soochow University, Suzhou, Jiangsu 215004, China;

<sup>3</sup>Department of Respiratory Medicine, Affiliated Jiangyin Hospital of Southeast University Medical College, Jiangyin, Jiangsu 214400, China;

<sup>4</sup>Department of Pathology, Affiliated Jiangyin Hospital of Southeast University Medical College, Jiangyin, Jiangsu 214400, China

\*These authors contributed equally to this work

**Background:** Recently, various dynamically expressed lncRNAs are known to play critical roles in cancer progression. Small nucleolar RNA host genes (SNHG), a stable cytoplasmic lncRNA, which have been widely reported to act as an oncogene in non-small cell lung cancer (NSCLC). As an important member of SNHG, SNHG8 have been suggested to over-expressed in several cancer disease, while the biological function in NSCLC remains unclear.

**Purpose:** Here we investigated the biological function and underlying mechanism of SNHG8 in human NSCLC.

**Patients and methods:** The relationship between SNHG8 expression and clinicopathologic characteristic in NSCLC patients were observed from January 2014 to December 2014 in 120 NSCLC patients. The expression of SNHG8 were analyzed by qRT-PCR assay in cancer tissues and cells. Cell proliferation ability were detected in NSCLC cells by CCK-8 assay. Flow cytometric analysis were performed to detected the cell apoptosis and cell cycle. Luciferase assay and Western blot assay were performed on NSCLC cells to detected the underlying mechanism of SNHG8 in NSCLC. Moreover, Tumor xenografts in nude mice were performed to detected the in vivo function of SNHG8.

**Results:** SNHG8 was over-expressed in NSCLC tissues and cells. Patients with high SNHG8 expression have poorer overall survival (OS) and progression-free survival (PFS) than the patients with low SNHG8 expression. SNHG8 knockdown inhibited NSCLC cell proliferation in vitro and in vivo, arrested cell cycle in the G0/G1 phase via targeting miR-542-3p/CCND1/CDK6, and induced cell apoptosis via activation of Caspase-3.

**Conclusion:** SNHG8 negatively regulated miR-542-3p in NSCLC progression by regulating downstream effectors including CCND1 and CDK6. SNHG8 showed great potential for the application in the treatment of NSCLC.

**Keywords:** SNHG8, non-small-cell lung cancer, cell proliferation, miR-542-3p, CCND1/CDK6, Caspase-3, cell proliferation, therapeutic target

## Introduction

Lung cancer remains the second most common cancer expected to occur and the first leading cause of death in both men and women in the US, with an estimated 1,735,350 new cases (856,370 among men and 879,980 among women) and 609,640 disease-related deaths (323,630 among men and 286,010 among women) in 2018.<sup>1</sup> Lung cancer accounts for 25% of all cancer deaths. Lung cancer is the main cause of cancer-related mortality, with about 733,300 new cases and 610,200 disease-related deaths reported in China.<sup>2</sup>

Non-small-cell lung cancer (NSCLC) accounts for nearly 80%–85% of lung cancer, while small cell lung cancer accounts for 15%–20% of lung cancer.<sup>3</sup> Unfortunately, most patients are diagnosed at the advanced-stage and the 5-year survival rate is only 2%, which is much lower than the rate of all stages of lung cancer.<sup>4</sup> Therefore, a better

Correspondence: Yuejun Sun  
Department of Pathology, Affiliated Jiangyin Hospital of Southeast University Medical College, No.163, shoushan road, Jiangyin, Jiangsu 214400, China  
Tel/fax: 0370-3256392  
Email yuejunsunjiangyin@163.com

understanding of the mechanisms of NSCLC progression and a new therapeutic target will contribute to disease treatment.

Recently, lncRNAs targeting protein-coding genes have been proved to be an important class of regulatory molecules.<sup>5,6</sup> As a subgroup of non-coding RNAs whose length is >200 nucleotides, lncRNA used to be treated as “transcriptional noise” without biological functions,<sup>7</sup> while various dynamically expressed lncRNAs are known to play critical roles in gene regulation, human pluripotent stem cell reprogramming, cellular homeostasis, and muscle differentiation.<sup>8–10</sup> Nowadays, the significant role of lncRNAs has been reported in a number of cancers. For example, the lncRNA POU3F3 was reported as a diagnostic marker in esophageal squamous cell carcinoma.<sup>11</sup> The lncRNA SNHG15 has been reported to be a potential prognostic marker of hepatocellular carcinoma, and overexpressed lncRNA SNHG15 represented worse survival rate.<sup>12</sup> Moreover, the lncRNA Linc00974 was found to be overexpressed in hepatocellular carcinoma, and silencing of Linc00974 inhibited tumor cell proliferation and invasion with activation of apoptosis and cell cycle arrest.<sup>13</sup> The lncRNA HOTAIR was found to be associated with various cancers including cancers of breast, liver, gastric, lung, and esophagus.<sup>14,15</sup> Thus, lncRNA has a great therapeutic potential not only as a biomarker, but also as a therapeutic target.

Here, we have attempted to elucidate the oncogenic role of lncRNA SNHG8 in NSCLC and have studied SNHG8 as a novel therapeutic target.

## Patients and methods

### Tissue collection

One hundred and twenty cancer tissues and paired adjacent non-tumor tissues were collected from NSCLC patients admitted in the Second Hospital of Nanjing, the Second Affiliated Hospital of Soochow University and the affiliated Jiangyin Hospital of Southeast University Medical College from January 2014 to December 2014. All patients were diagnosed based on histopathologic evaluation, and none of these patients had received any radiotherapy or chemotherapy before surgery. Overall survival (OS) was defined as the time interval between surgery and death. Progression-free survival (PFS) was defined as the time interval between surgery and tumor progression or death. The characteristics of NSCLC patients were obtained from their clinicopathologic reports and are presented in Table 1. All patients had carried out a follow-up every month, which ranged from 2 to 60 months since the day of surgery. All patients signed informed consent, and all experiments were approved by the ethics committee of the Second Hospital of Nanjing.

**Table 1** Relationship of SNHG8 expression with clinicopathologic characteristics in NSCLC patients

	Number of patients	SNHG8 expression		P-value
		Low	High	
All patients	120	51	69	
Gender				0.553
Male	65	28	37	
Female	55	22	33	
Age				0.345
<65 years	68	31	37	
≥65 years	52	20	32	
Size of tumor				0.501
≤3 cm	43	17	26	
>3 cm	77	33	44	
Grade				0.192
Low	16	9	7	
High	104	41	63	
Lymph node metastasis				0.0402*
N0	52	28	24	
N1–3	68	23	45	
TNM stages				0.0221*
I–II	40	23	17	
III–IV	80	28	52	

**Note:** \* $P < 0.05$ .

**Abbreviation:** NSCLC, non-small-cell lung cancer.

### Cell culture and transfection

Four human NSCLC cell lines (A549, H23, SPC-A1, and NCI-H292) and one human bronchial epithelial cell line (16HBE) were obtained from the Institute of Biochemistry and Cell Biology of the Chinese Academy of Sciences (Shanghai, China). Cells were incubated in RPMI-1640 (Thermo Fisher Scientific, Waltham, MA, USA) with 10% fetal bovine serum (Thermo Fisher Scientific), 100 U/mL penicillin, and 100 mg/mL streptomycin (Thermo Fisher Scientific) at 37°C in a 5% CO<sub>2</sub> atmosphere.

For knockdown of SNHG8, SNHG8 siRNA (SNHG8 siRNA1, SNHG8 siRNA2, SNHG8 siRNA3) and negative control (NC) SNHG8 were purchased from Thermo Fisher Scientific and kept at –80°C. For overexpression of miR-542-3p, miR-542-3p mimic and NC-miR-542-3p were purchased from Thermo Fisher Scientific, too. After 50%–60% confluence was achieved, cells were transfected with lentivirus, respectively. Then the media were replaced with fresh media after 24 hours. Subsequent experiments were performed after the next 24–96 hours according to the manufacturer’s instructions.

### RNA extraction and quantitative real-time-polymerase chain reaction (qRT-PCR) assays

Total RNA was isolated using Trizol (Thermo Fisher Scientific), and reverse transcription was performed using

cDNA Reverse Transcription kit (Takara, Dalian, China). qRT-PCR was carried out with SYBR Green Kit (Thermo Fisher Scientific) on ABI 7500 real-time polymerase chain reaction system. The gene expressions were calculated using the  $2^{-\Delta\Delta Ct}$  method, with  $\beta$ -actin as an internal control. All reactions were repeated three times. The sequences of real-time polymerase chain reaction primers were as follows: SNHG8, forward 5'-TGTAAGCTCCTTCTCGGGGCG-3' and reverse 5'-GTCTATTTCTGGTGAATTTGG-3'.

### Plasmids construction and luciferase assay

Dual-luciferase miRNA target expression vector in SNHG8 containing the predicted miR-542-3p binding site (SNHG8-Wt) and with the mutated miR-542-3p binding site (SNHG8-Mut) were obtained. Then Luc-SNHG8-wt and Luc-SNHG8-mut were co-transfected separately with miR-542-3p into HEK293T cells using Lipofectamine 2000 (Thermo Fisher Scientific). The pmirGLO control vector was transfected and it served as a control. Firefly and Renilla luciferase activities were measured in cell lysates 48 hours after transfection following the manufacturer's protocol (Promega Corporation, Fitchburg, WI, USA).

### Western blot analysis

Protein was extracted with RIPA buffer from tissues or cell lysates, and the protein concentration was determined using a BCA Protein Assay Kit (Thermo Fisher Scientific). Protein lysates were isolated by sodium dodecyl sulfate-polyacrylamide gel electrophoresis, moved to a polyvinylidene difluoride membrane, and immunoblotted with the following antibodies: CCND1, CDK6, Caspase-3 (1:1,000 dilution; Cell Signaling Technology, Inc., Danvers, MA, USA), or GADPH (1:2,000; Santa Cruz Biotechnology Inc., Dallas, TX, USA) overnight at 4°C. After washing, the membrane was incubated with HRP-conjugated goat anti-rabbit IgG goat anti-mouse (1:10,000; Santa Cruz Biotechnology Inc.) or goat anti-rabbit (1:10,000; Santa Cruz Biotechnology Inc.) antibody for 2 hours at room temperature. Protein bands were detected by enhanced chemiluminescence (GE Healthcare Life Sciences, Little Chalfont, UK). GADPH served as a loading control.

### Cell proliferation assays

Exactly  $1.0 \times 10^3$  cells per well were plated into 96-well plates (Corning Incorporated, Corning, NY, USA) for 24 hours, and then cell proliferation was detected using the Cell Counting Kit-8 (CCK-8) kit (MedChemExpress, Monmouth Junction, NJ, USA) according to the manufacturer's instructions. Briefly, 10  $\mu$ L of CCK-8 was added to each well at 24, 48, and 72 hours after transfection; then, the cells were incubated at room temperature for another 2 hours and the absorbance was measured at 450 nm.

### Flow cytometric analysis of apoptosis and the cell cycle

Exactly  $1 \times 10^5$  cells per well were seeded in 24-well plates and were fixed with 70% cold ethanol after 48 hours. Two hours later, the fixed cells with 100  $\mu$ L of RNase (BD Biosciences, San Jose, CA, USA) were incubated at 37°C for 30 minutes. Subsequently, 400  $\mu$ L of propidium iodide was added and cells were kept in a dark place at 4°C for 0.5 hour. Similarly,  $1 \times 10^5$  cells per well were seeded in 24-well plates; after 48 hours, the apoptotic cells were determined using fluorescein isothiocyanate-Annexin V Apoptosis Detection Kit (BD Biosciences). Cell cycle and apoptosis were assayed with flow cytometry (FACScan; BD Biosciences). All experiments were done in triplicate and repeated independently three times.

### Tumor xenografts in nude mice

Five-week-old male BALB/c nude mice were obtained from the Southeast University Laboratory Animal Center (Nanjing, China). All experiments were performed in accordance with the UK Animals (Scientific Procedures) Act 1986 and associated guideline and were approved by the Southeast University Laboratory Animal Center Commission. Exactly  $1 \times 10^7$  A549 cells/mL stably transfected with lv-shSNHG8 or negative vector were subcutaneously injected into the left side of the posterior flank of BALB/c nude mice. Mice weight and tumor volume were measured every 7 days. Tumor volumes were calculated as  $L \times W^2 \times 0.5$ , where L is tumor length and W is tumor width. Twenty-eight days after injection, all mice were sacrificed, tumors were weighed and immediately snap frozen in liquid nitrogen, and stored at  $-80^\circ\text{C}$  until use.

### Statistical analysis

All statistical evaluations were performed with GraphPad Prism 6.0 software (GraphPad Software, Inc., La Jolla, CA, USA). Data were expressed as mean  $\pm$  SD. Statistically significant differences between groups were estimated by Student's *t*-test. SNHG8 expression levels between NSCLC tissues and normal tissues were determined using *t*-test and one-way analysis of variance. Survival analysis was performed by Kaplan–Meier procedure, and the log-rank test was performed to evaluate the difference between survival curves.  $P < 0.05$  was defined statistically significant.

## Results

### SNHG8 is upregulated and associated with poor prognosis of NSCLC

To identify upregulation of SNHG8 in NSCLC, we performed qRT-PCR assay on 120 cancer tissues and paired

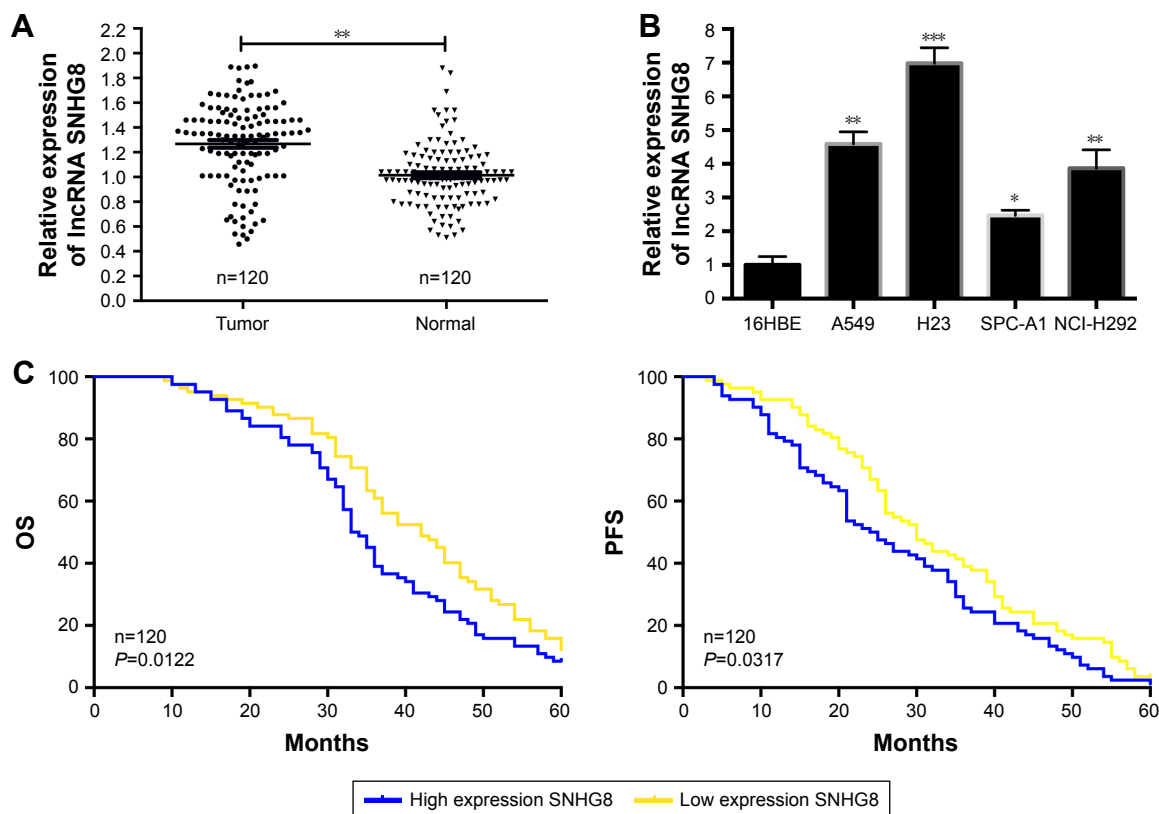


**Figure 1** SNHG8 is upregulated and associated with poor prognosis of NSCLC.

**Notes:** (A) Expression of SNHG8 in 120 pairs of NSCLC tissues and paired adjacent normal lung tissues. (B) Expression of SNHG8 in four human NSCLC cell lines (A549, H23, SPC-A1, and NCI-H292) and one human bronchial epithelial cell line (16HBE). (C) The Kaplan–Meier OS and PFS curves of SNHG8 levels. \* $P < 0.05$ , \*\* $P < 0.01$ , and \*\*\* $P < 0.001$ .

**Abbreviations:** NSCLC, non-small-cell lung cancer; OS, overall survival; PFS, progression-free survival.

adjacent non-tumor tissues, one human bronchial epithelial cell line, and four NSCLC cell lines. Our findings showed that SNHG8 expression was ubiquitously higher in cancer tissues than in adjacent non-tumor tissues ( $P < 0.01$ ; Figure 1A). Besides, SNHG8 expression was much higher in cancer cell lines than in normal bronchial epithelial cell line ( $P < 0.05$ ; Figure 1B), especially in A549 and H23 cell lines. Furthermore, we divided all NSCLC tissue samples into two groups according to the median mRNA level of SNHG8 as the cutoff value (high SNHG8 expression group: SNHG8 mRNA expression ratio  $>$  median mRNA level; low SNHG8 expression group: SNHG8 mRNA expression ratio  $\leq$  median mRNA level). As Table 1 shows, SNHG8 overexpression had a significant correlation with lymph node metastasis ( $P = 0.0402$ ) and TNM stages ( $P = 0.0221$ ). Moreover, high expression of SNHG8 predicted poor prognosis in NSCLC. Patients in the high SNHG8 expression group had significantly shorter OS and PFS than those in the low SNHG8 group ( $P < 0.05$ ; Figure 1C). Thus, these results

show that upregulated expression of SNHG8 in NSCLC significantly decreases the patients' survival time.

## SNHG8 promotes NSCLC cells proliferation

To explore the oncogenic activity and role of SNHG8 in NSCLC, we successfully established NSCLC cells with SNHG8 transient knockdown in mRNA. Interference efficiency of SNHG8 siRNA1, SNHG8 siRNA2, and SNHG8 siRNA3 was evaluated by qRT-PCR after transfection in A549 and H23 cells. We found that both siRNAs obviously downregulated the mRNA level of SNHG8, of which the inhibitory effect of siRNA1 was more significant ( $P < 0.05$ ; Figure 2A). So, we selected siRNA1 for subsequent functional verification. Then, we performed CCK-8 assays which showed that SNHG8 knockdown significantly attenuated the vitality of A549 and H23 cells ( $P < 0.05$ ; Figure 2B). The decrease in proliferation was much higher in A549 cell than in other cells, so we performed the follow-up analysis on A549 cells.

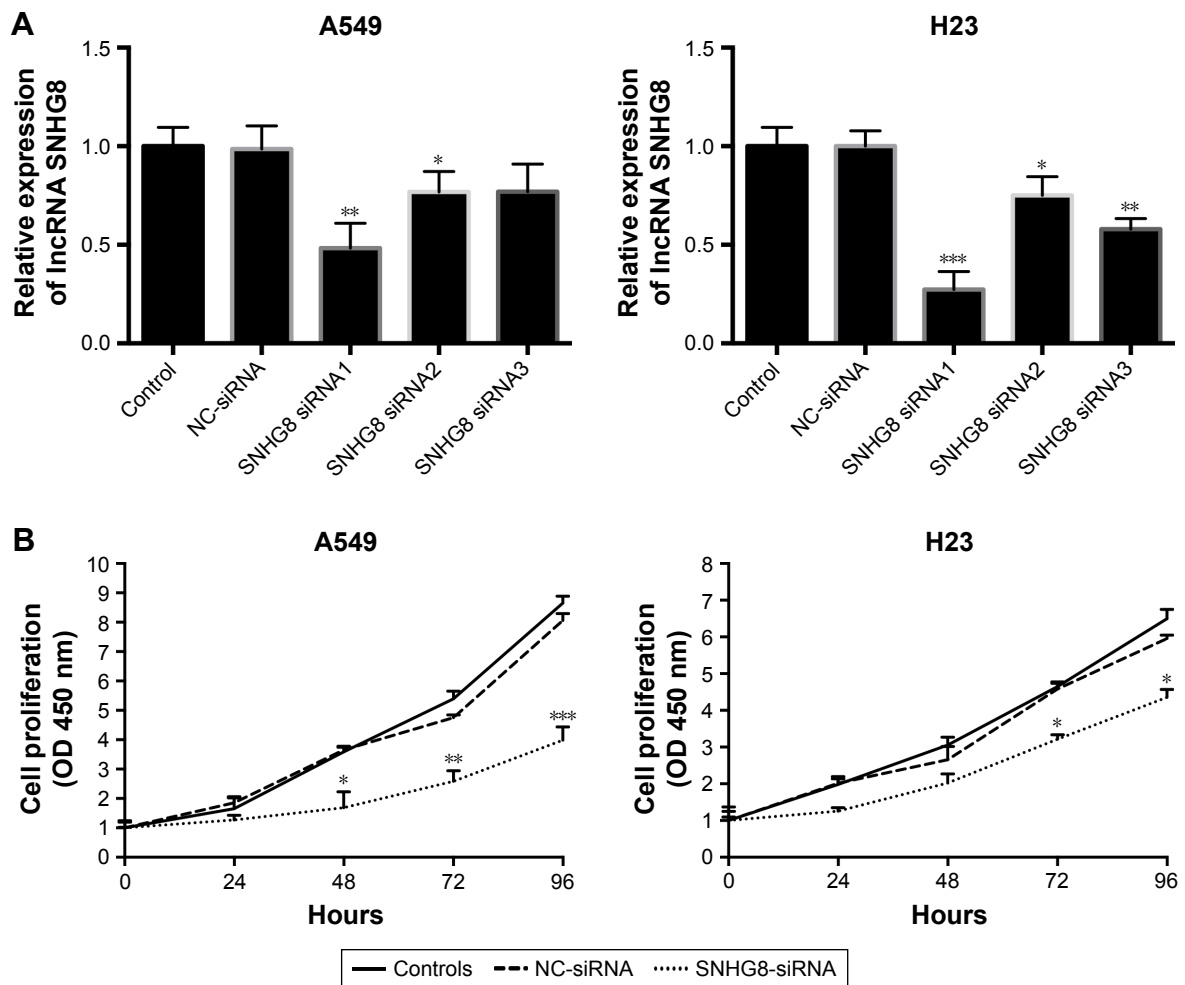


**Figure 2** SNHG8 promotes NSCLC cells proliferation.

**Notes:** (A) Interference efficiency of SNHG8 siRNA1, SNHG8 siRNA2, and SNHG8 siRNA3 was evaluated by qRT-PCR after transfection in A549 and H23 cells. (B) The effects of SNHG8 knockdown on the vitality of NSCLC cells was measured using the CCK-8 assay. \* $P < 0.05$ , \*\* $P < 0.01$ , and \*\*\* $P < 0.001$ .

**Abbreviations:** CCK-8, Cell Counting Kit-8; NC, negative control; NSCLC, non-small-cell lung cancer; qRT-PCR, quantitative real-time-polymerase chain reaction.

## SNHG8 exerted its function through sponging miR-542-3p

To investigate the underlying mechanism of SNHG8 in NSCLC cells, we examined the potential miRNAs associated with SNHG8 because lncRNAs function mainly as miRNA sponges. With starBase version 2.0,<sup>16,17</sup> miR-542-3p turned out to be the possible target of SNHG8. The putative binding sites of miR-542-3p and wild-type regions of SNHG8 are shown in Figure 3A. Dual-luciferase reporter assay was performed to explore whether SNHG8 was a functional target of miR-542-3p. As shown in Figure 3B, the luciferase activity was significantly reduced in miR-542-3p mimics and SNHG8-Wt co-transfected HEK293T cells, which had no effect on the SNHG8-Mut vector ( $P < 0.05$ ). In addition, qRT-PCR analysis showed that silencing of SNHG8 significantly increased miR-542-3p expression ( $P < 0.001$ ;

Figure 3C). However, overexpression of miR-542-3p was not found to affect SNHG8 expression ( $P > 0.05$ ; Figure 3D). Taken together, these results indicated that miR-542-3p was an inhibitory target for SNHG8 in NSCLC progression.

## SNHG8 depletion arrested cell cycle in the G0/G1 phase via targeting miR-542-3p/CCND1/CDK6

We then examined the impact of decreased SNHG8 on cell cycle in A549 cells. Flow cytometric analysis showed a decrease in the percentage of cells in the G2/M phase and a marked accumulation of cells in the G0/G1 phase in the SNHG8 siRNA group compared with control and NC-siRNA groups ( $P < 0.01$ ; Figure 4A). These results indicated that downregulation of SNHG8 expression in A549 cells was arrested in the G0/G1 phase. miR-542-3p has been

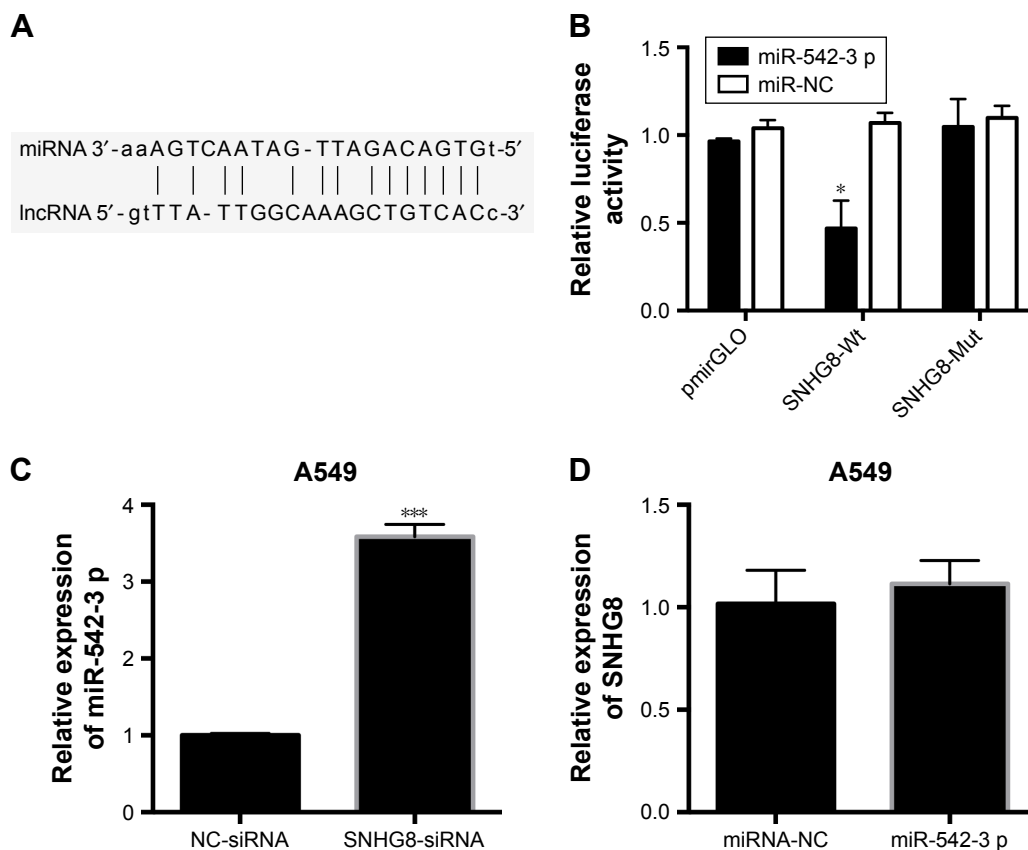


**Figure 3** SNHG8 exerted its function through sponging miR-542-3p.

**Notes:** (A) Sequence alignment of miR-542-3p with the putative binding sites in the wild-type regions of SNHG8. (B) Dual-luciferase reporter assay showed that miR-542-3p mimics reduced the intensity of fluorescence in HEK293T cells transfected with SNHG8-Wt instead of SNHG8-Mut vector. (C) qRT-PCR analysis of miR-542-3p expression in A549 cells transfected with siRNA-SNHG8 or siRNA-NC. (D) qRT-PCR analysis of SNHG8 expression in A549 cells transfected with miR-542-3p or miR-NC. \* $P < 0.05$ , \*\*\* $P < 0.001$ .

**Abbreviations:** NC, negative control; qRT-PCR, quantitative real-time-polymerase chain reaction.

proved to induce G1 phase arrest of cell cycle in human A549 cells, which seemed to occur by downregulating CDK 6 in the G1/S phase.<sup>18</sup> To analyze whether miR-542-3p regulated the G1 phase cell cycle genes, we transfected A549 cells with miR-542-3p mimics. As Figure 4B shows, overexpression of miR-542-3p led to a significant decrease in endogenous cyclin D1 (CCND1) and CDK6 proteins at the protein level. Meanwhile, knockdown of SNHG8 caused a similar induction of the expression of CCND1 and CDK6 (Figure 4C). These data indicate that miR-542-3p downregulated the expressions of CCND1 and CDK6 at the translational level.

SNHG8 depletion reduced cell apoptosis via activation of Caspase-3. In order to determine the effects of SNHG8 depletion on apoptosis, Annexin V/propidium iodide double staining was performed on A549 cells. It was found that depletion of SNHG8 largely promoted late apoptosis (Figure 5). Statistical analysis revealed that ~10-fold and 7-fold increase of late apoptotic populations was detected in SNHG8 siRNA-infected A549 cells (45.1%±0.49%), as

compared to NC siRNA-infected and control A549 cells (4.49%±0.08% and 6.46%±0.10%, respectively,  $P < 0.001$ ; Figure 5B). To confirm the apoptosis effect, we examined the protein expression of Caspase-3, which was related to apoptosis, and the results showed that Caspase-3 level was upregulated in SNHG8 siRNA group cells compared to NC-siRNA group cells and control group cells in A549 cells (Figure 5C). These results indicated SNHG8 knockdown could induce apoptosis via activation of Caspase-3 in NSCLC cells.

## SNHG8 promotes growth of NSCLC tumors in vivo

To further confirm the oncogenic activity of SNHG8, we inoculated A549 cells transfected with SNHG8-siRNA or NC-siRNA into nude mice. All mice developed xenograft tumors at the injection site. As shown in Figure 6A and B, tumor growth in SNHG8-siRNA group was significantly lower than that in NC-siRNA group ( $P < 0.05$ ), while the weight of mice changed a little ( $P > 0.05$ ). After the mice were

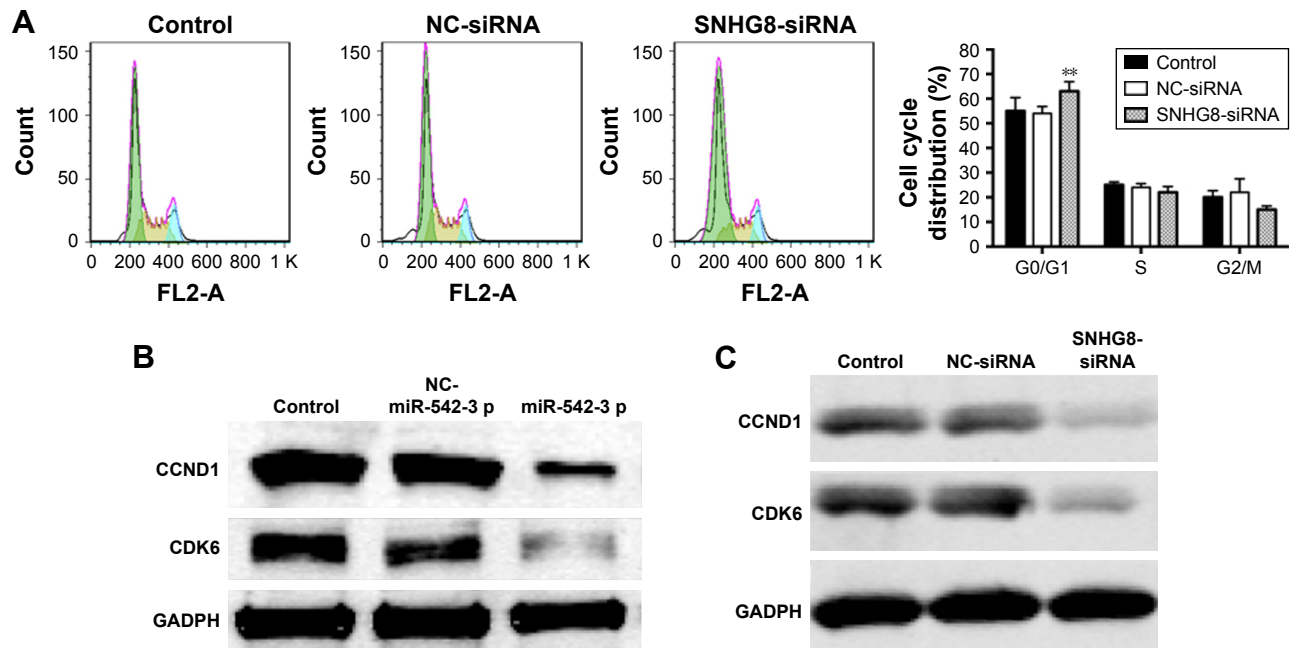


**Figure 4** SNHG8 depletion arrested cell cycle in the G0/G1 phase via targeting miR-542-3p/CCND1/CDK6. **Notes:** (A) Depletion of SNHG8 in A549 cells led to an increase of cells at the G0/G1 phase and a concomitant decrease of cells at the G2/M phase. (B) CCND1 and CDK6 proteins in A549 cells were measured by Western blot at 48 hours post-transfection with different treatments (control, NC-miR-542-3p, or miR-542-3p). GADPH was used as an internal loading control. (C) CCND1 and CDK6 proteins in A549 cells were measured by Western blot at 48 hours post-transfection with different treatments (control, NC-siRNA, or SNHG8-siRNA). GADPH was used as an internal loading control. **\*\*P**<0.01. **Abbreviations:** NC, negative control; GADPH, Glyceraldehyde-3-phosphate dehydrogenase.

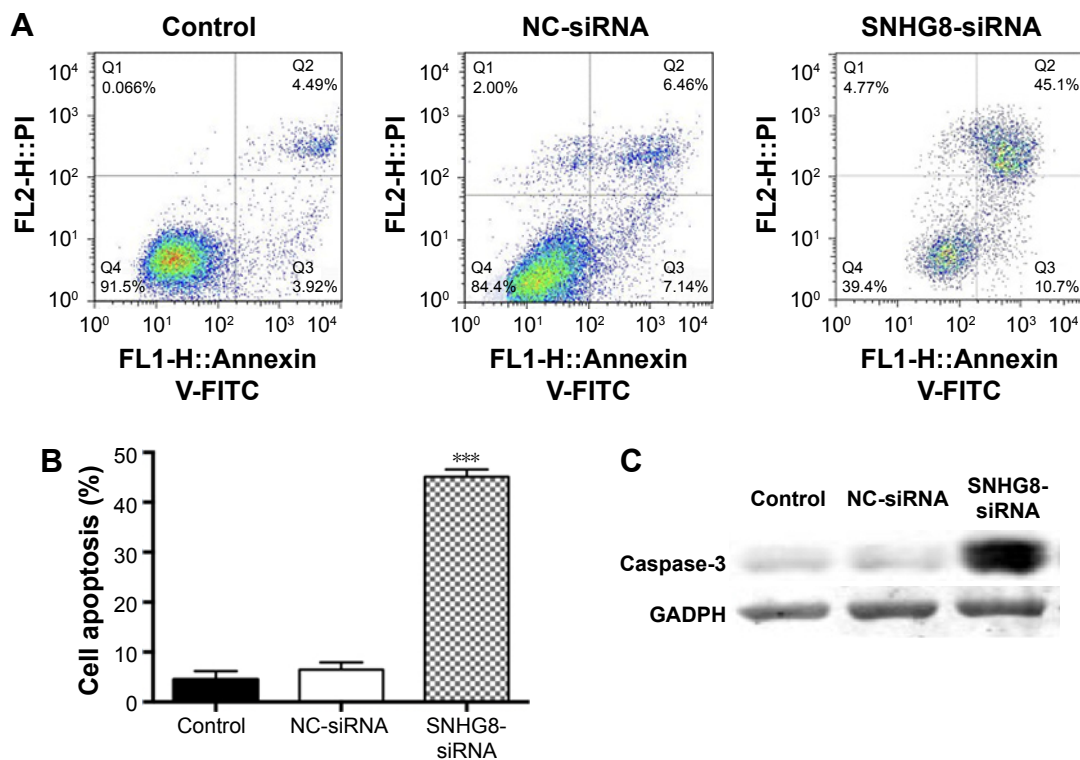


**Figure 5** SNHG8 depletion reduced cell apoptosis via activation of Caspase-3. **Notes:** (A) Apoptotic cells were assessed by Annexin V/PI double staining and then subjected to flow cytometry analysis. Representative images showing results of Annexin V/PI staining in A549 cells with different treatments (control, NC-siRNA, or SNHG8-siRNA). (B) Detection of apoptosis 48 hours after transfection with siRNA using FCM analysis. (C) Caspase-3 proteins in A549 cells were measured by Western blot at 48 hours post-transfection with different treatments (control, NC-siRNA, or SNHG8-siRNA). GADPH was used as an internal loading control. **\*\*\*P**<0.001. **Abbreviations:** FCM, flow cytometry; FITC, fluorescein isothiocyanate; NC, negative control; PI, propidium iodide.

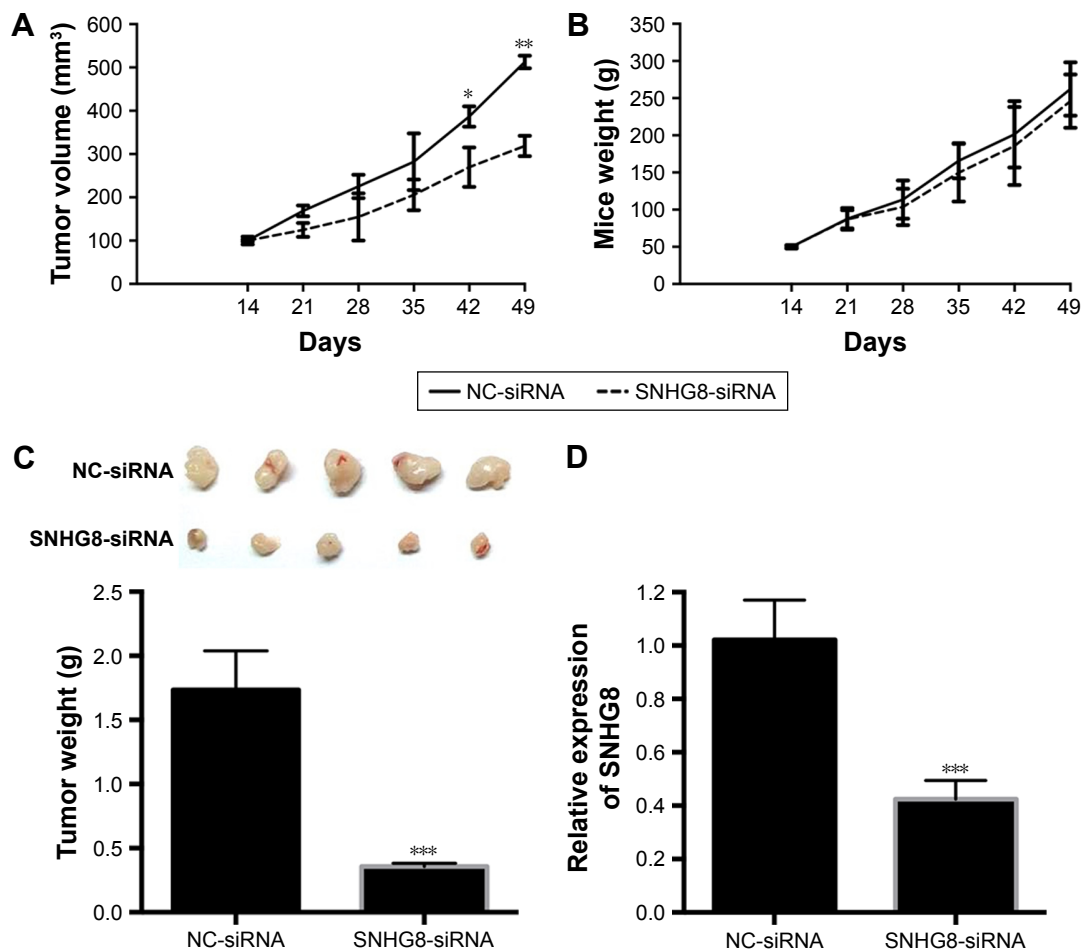


**Figure 6** SNHG8 promotes the growth of NSCLC tumors in vivo.

**Notes:** (A) Tumor volume of subcutaneous implantation models of A549 cells transfected with SNHG8-siRNA or NC-siRNA. (B) The weight of mice in SNHG8-siRNA or NC-siRNA group. (C) Tumors were collected and weighed after the mice were sacrificed. (D) SNHG8 mRNA expression in the tumor tissues was measured with different treatments (NC-siRNA or SNHG8-siRNA). GAPDH was used as an internal loading control. n=5. \* $P<0.05$ , \*\* $P<0.01$  and \*\*\* $P<0.001$ .

**Abbreviations:** NC, negative control; NSCLC, non-small-cell lung cancer.

sacrificed, we found the average tumor weight in the SNHG8-siRNA group was obviously lower than in NC-siRNA group ( $P<0.001$ ; Figure 6C). qRT-PCR assays revealed that the expression level of SNHG8 was much lower in SNHG8-siRNA group ( $P<0.001$ ; Figure 6D). Taken together, these results indicate that SNHG8 can inhibit the proliferation capacity of NSCLC cells in vivo.

Altogether, the above results show that SNHG8 “sponged” miR-542-3p in NSCLC to regulate the expression of CCND1 and CDK6, functional genes that reduced cell cycle arrest (Figure 7).

## Discussion

Several studies have suggested that lncRNAs are related to tumor initiation and progression and are thought of as being therapeutic and prognostic markers for various types of cancer, including NSCLC.<sup>19</sup> Small nucleolar RNA host genes (SNHG), stable cytoplasmic lncRNAs, have been

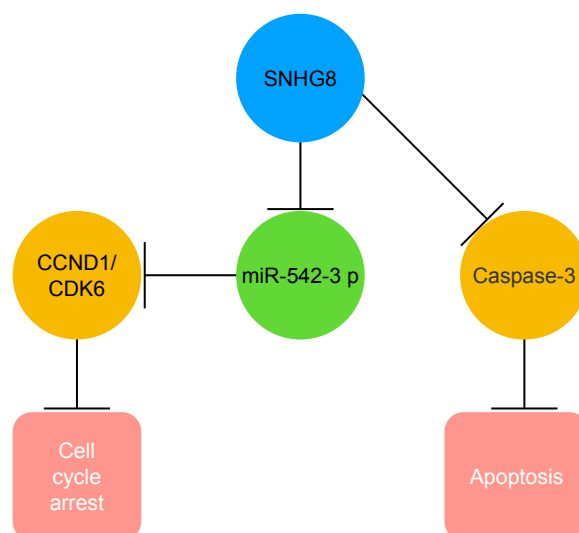


**Figure 7** Schematic representation of the circuitry linking SNHG8, miR-542-3p, CCND1/CDK6, and cell cycle arrest or cell apoptosis.

**Note:** “SNHG8–miR-542-3p–CCND1/CDK6” axis played a critical role in the regulatory interactions governing NSCLC progression.

**Abbreviation:** NSCLC, non-small-cell lung cancer.



widely reported to be overexpressed in NSCLC and promote NSCLC initiation and progression. For example, Cui et al showed that SNHG1 was upregulated in NSCLC tissues and cells, and it promoted the progression of NSCLC via SNHG1/miR-101-3 p/SOX9/Wnt/ $\beta$ -catenin axis.<sup>20</sup> She et al identified that upregulated SNHG7 was involved in NSCLC cell proliferation and metastasis and led to impaired miR-193b/FAIM2-induced tumor progression.<sup>21</sup>

SNHG8, an important member of SNHG, has been suggested to act as an oncogene, but the underlying mechanism by which SNHG8-mediated gene expression participates in NSCLC progression remains unclear. Much of the research and evidence about SNHG8 focused on Epstein–Barr virus (EBV)-associated gastric carcinoma. Huang et al demonstrated that SNHG8 lncRNA level in EBV-associated gastric carcinoma was significantly higher than that in the adjacent tissue<sup>22</sup> and validated SNHG8 as the target gene of EBV through sequencing lncRNA–mRNA co-expression network. Yang et al demonstrated that SNHG8 lncRNA level in endometrial carcinoma tissue was markedly higher than that in normal endometrium.<sup>23</sup> Based on the analysis of lncRNA–mRNA co-expression network and lncRNA–miRNA sponges, we concentrated on the potential lncRNA–microRNA–mRNA co-expression network of SNHG8 in NSCLC, which would be meaningful for future development of novel treatments.

In this study, we detected the expression of SNHG8 in NSCLC and the adjacent normal lung tissue samples and found that SNHG8 was overexpressed in NSCLC tissues in comparison with surrounding non-tumorous tissues. Kaplan–Meier analysis showed that the patients with high SNHG8 expression had poorer OS and PFS than the patients with low SNHG8 expression. Moreover, we performed several experiments to explore the oncogenic function in NSCLC and found that SNHG8 promoted NSCLC cell proliferation in vivo and in vitro. We identified miR-542-3p as the inhibited target of SNHG8 depletion and miR-542-3p overexpression arrested cell cycle in the G0/G1 phase by inhibiting the expressions of CCND1 and CDK6 at the translational level. Cell apoptosis assays revealed that SNHG8 depletion reduced cell apoptosis via Caspase-3 activation. These findings suggest that SNHG8 negatively regulates miR-542-3p in NSCLC progression by regulating downstream effectors including CCND1 and CDK6. Cell cycle growth inhibition is an attractive target for anticancer therapy, and SNHG8/miR-542-3p has the potential for application in the treatment of cancers. In future, identification of more targets of SNHG8/miR-542-3p might be a new research direction and therapeutic approach in NSCLC.

## Disclosure

The authors report no conflicts of interest in this work.

## References

1. Siegel RL, Miller KD, Jemal A. Cancer statistics, 2018. *CA Cancer J Clin.* 2018;68(1):7–30.
2. Chen W, Zheng R, Baade PD, et al. Cancer statistics in China, 2015. *CA Cancer J Clin.* 2016;66(2):115–132.
3. Reck M, Popat S, Reinmuth N, et al. Metastatic non-small-cell lung cancer (NSCLC): ESMO Clinical Practice Guidelines for diagnosis, treatment and follow-up. *Ann Oncol.* 2014;25(Suppl 3):iii27–iii39.
4. Ettinger DS, Wood DE, Akerley W, et al. NCCN guidelines insights: non-small cell lung cancer, version 4.2016. *J Natl Compr Canc Netw.* 2016;14(3):255–264.
5. Yarmishyn AA, Kurochkin IV. Long noncoding RNAs: a potential novel class of cancer biomarkers. *Front Genet.* 2015;6:145.
6. Deng R, Liu B, Wang Y, et al. High expression of the newly found long noncoding RNA Z38 promotes cell proliferation and oncogenic activity in breast cancer. *J Cancer.* 2016;7(5):576–586.
7. Kung JT, Colognori D, Lee JT. Long noncoding RNAs: past, present, and future. *Genetics.* 2013;193(3):651–669.
8. Sheik Mohamed J, Gaughwin PM, Lim B, Robson P, Lipovich L. Conserved long noncoding RNAs transcriptionally regulated by Oct4 and Nanog modulate pluripotency in mouse embryonic stem cells. *RNA.* 2010;16(2):324–337.
9. Guttman M, Donaghey J, Carey BW, et al. lincRNAs act in the circuitry controlling pluripotency and differentiation. *Nature.* 2011;477(7364):295–300.
10. Yang L, Froberg JE, Lee JT. Long noncoding RNAs: fresh perspectives into the RNA world. *Trends Biochem Sci.* 2014;39(1):35–43.
11. Tong Y-S, Wang X-W, Zhou X-L, et al. Identification of the long non-coding RNA POU3F3 in plasma as a novel biomarker for diagnosis of esophageal squamous cell carcinoma. *Mol Cancer.* 2015;14(1):3–13.
12. Zhang JH, Wei HW, Yang HG. Long noncoding RNA SNHG15, a potential prognostic biomarker for hepatocellular carcinoma. *Eur Rev Med Pharmacol Sci.* 2016;20(9):1720–1724.
13. Tang J, Zhuo H, Zhang X, et al. A novel biomarker Linc00974 interacting with KRT19 promotes proliferation and metastasis in hepatocellular carcinoma. *Cell Death Dis.* 2014;5(12):e1549.
14. Liu X, Liu Z, Sun M, Liu J, Wang Z, Wei D. The long non-coding RNA HOTAIR indicates a poor prognosis and promotes metastasis in non-small cell lung cancer. *BMC Cancer.* 2013;13(1):464.
15. Bhan A, Mandal SS. LncRNA HOTAIR: a master regulator of chromatin dynamics and cancer. *Biochim Biophys Acta.* 2015;1856(1):151–164.
16. Yang JH, Li JH, Shao P, et al. starBase: a database for exploring microRNA–mRNA interaction maps from Argonaute CLIP-Seq and Degradome-Seq data. *Nucleic Acids Res.* 2011;39(Database issue):D202–D209.
17. Jh L, Liu S, Zhou H, Lh Q, Yang JH. starBase v2.0: decoding miRNA–ceRNA, miRNA–ncRNA and protein–RNA interaction networks from large-scale CLIP-Seq data. *Nucleic Acids Res.* 2014;42(Database issue):D92.
18. Yoon S, Choi YC, Lee S, Jeong Y, Yoon J, Baek K. Induction of growth arrest by miR-542-3p that targets survivin. *FEBS Lett.* 2010;584(18):4048–4052.
19. Prensner JR, Chinnaiyan AM. The emergence of lncRNAs in cancer biology. *Cancer Discov.* 2011;1(5):391–407.
20. Cui Y, Zhang F, Zhu C, Geng L, Tian T, Liu H. Upregulated lncRNA SNHG1 contributes to progression of non-small cell lung cancer through inhibition of miR-101-3p and activation of Wnt/ $\beta$ -catenin signaling pathway. *Oncotarget.* 2017;8(11):17785–17794.
21. She K, Yan H, Huang J, Zhou H, He J. miR-193b availability is antagonized by lncRNA-SNHG7 for FAIM2-induced tumour progression in non-small cell lung cancer. *Cell Prolif.* 2018;51(1):e12406.

22. Huang T, Ji Y, Hu D, et al. SNHG8 is identified as a key regulator of Epstein–Barr virus (EBV)-associated gastric cancer by an integrative analysis of lncRNA and mRNA expression. *Oncotarget*. 2016;7(49): 80990–81002.
23. Yang CH, Zhang XY, Zhou LN, et al. LncRNA SNHG8 participates in the development of endometrial carcinoma through regulating c-MET expression by miR-152. *Eur Rev Med Pharmacol Sci*. 2018;22(6): 1629–1637.

### OncoTargets and Therapy

## Publish your work in this journal

OncoTargets and Therapy is an international, peer-reviewed, open access journal focusing on the pathological basis of all cancers, potential targets for therapy and treatment protocols employed to improve the management of cancer patients. The journal also focuses on the impact of management programs and new therapeutic agents and protocols on

Submit your manuscript here: <http://www.dovepress.com/oncotargets-and-therapy-journal>

patient perspectives such as quality of life, adherence and satisfaction. The manuscript management system is completely online and includes a very quick and fair peer-review system, which is all easy to use. Visit <http://www.dovepress.com/testimonials.php> to read real quotes from published authors.

Dovepress